Direct observation of substitutional Ga after ion implantation in Ge by means of extended x-ray absorption fine structure

S. Decoster, B. Johannessen, C. J. Glover, S. Cottenier, T. Bierschenk et al.

Related Articles

Mechanisms of boron diffusion in silicon and germanium
App. Phys. Rev. 2013, 3 (2013)

Formation of Si or Ge nanodots in Si3N4 with in-situ donor modulation doping of adjacent barrier material
AIP Advances 3, 012109 (2013)

Mechanisms of boron diffusion in silicon and germanium
J. Appl. Phys. 113, 031101 (2013)

Experimental verification of intermediate band formation on titanium-implanted silicon
J. Appl. Phys. 113, 024104 (2013)

Efficient n-type doping of Si nanocrystals embedded in SiO2 by ion beam synthesis
Appl. Phys. Lett. 102, 013116 (2013)

Additional information on Appl. Phys. Lett.

Journal Homepage: http://apl.aip.org/

Journal Information: http://apl.aip.org/about/about_the_journal

Top downloads: http://apl.aip.org/features/most_downloaded

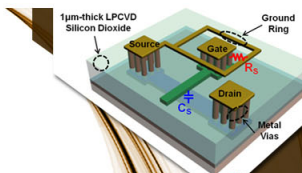Information for Authors: http://apl.aip.org/authors
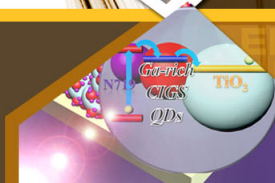
Direct observation of substitutional Ga after ion implantation in Ge by means of extended x-ray absorption fine structure

S. Decoster,[1,2,a)] B. Johannessen,[3] C. J. Glover,[3] S. Cottenier,[4] T. Bierschenk,[2] H. Salama,[2] F. Kremer,[2] K. Temst,[1] A. Vantomme,[1] and M. C. Ridgway[2]

[1]*Instituut voor Kern-en Stralingsfysica, KU Leuven, Celestijnenlaan 200D, 3001 Leuven, Belgium*
[2]*Australian National University, Research School of Physics and Engineering, Canberra, ACT 0200, Australia*
[3]*Australian Synchrotron, Clayton, VIC 3168, Australia*
[4]*Center for Molecular Modeling and Department of Materials Science and Engineering, Ghent University, Technologiepark 903, 9052 Zwijnaarde, Belgium*

We present an experimental lattice location study of Ga atoms in Ge after ion implantation at elevated temperature (250 °C). Using extended x-ray absorption fine structure (EXAFS) experiments and a dedicated sample preparation method, we have studied the lattice location of Ga atoms in Ge with a concentration ranging from 0.5 at. % down to 0.005 at. %. At Ga concentrations ≤ 0.05 at.%, all Ga dopants are substitutional directly after ion implantation, without the need for post-implantation thermal annealing. At higher Ga concentrations, a reduction in the EXAFS amplitude is observed, indicating that a fraction of the Ga atoms is located in a defective environment. The local strain induced by the Ga atoms in the Ge matrix is independent of the Ga concentration and extends only to the first nearest neighbor Ge shell, where a 1% contraction in bond length has been measured, in agreement with density functional theory calculations. © 2012 American Institute of Physics. [http://dx.doi.org/10.1063/1.4773185]

Boron has been the most extensively studied *p*-type dopant in Ge during the past decade. However, the low diffusivity and high solid solubility (4.9×10^{20}/cm^3) of Ga represent a promising alternative *p*-type dopant.[1] The activation of implanted Ga in Ge has been studied after rapid thermal annealing and flash annealing,[2,3] but so far, the maximum active Ga concentration of 6.6×10^{20}/cm^3 has been achieved by Impellizzeri *et al.* after conventional furnace annealing at $450 - 550\,°C$.[4] Higher temperature annealing ($\geq 600\,°C$) resulted in a drastic reduction of the active fraction, attributed to Ga clustering.[4,5] Besides being a promising electrical dopant, recent reports have shown that Ga implantation in Ge results in superconductivity, which makes this system even more topical.[6]

Despite several diffusion and activation studies on Ga-doped Ge, little is known about the atomic-scale structural configuration of the Ga atoms and their surroundings. This information is, however, crucial to understand the activation and clustering behavior of this system. Until now, no direct lattice location studies, e.g., by using electron channeling, ion channeling, or extended x-ray absorption fine structure (EXAFS) experiments, have been performed. Ion channeling experiments of Ga-doped Ge are impeded by the similar Z values of Ga and Ge and the resulting overlap of their backscattering signals. Indirect information on the lattice location of Ga in Ge has been extracted from deep level transient spectroscopy experiments, where two deep level signals which anneal out slightly above room temperature, have been attributed to interstitial Ga after low temperature electron irradiation of Ge.[7,8] Besides this indirect *experimental* result and the electrical activation studies which indicate that at least a fraction of the Ga atoms in Ge occupy the substitu-

tional (S) site, a *theoretical* study of the lattice relaxation around an isolated substitutional Ga atom and the Ga-monovacancy complex in Ge has shown that the Ga atom prefers the S site, even with a vacancy as nearest neighbor (NN), and that the distance to the first NN Ge atoms of substitutional Ga is 1.5% smaller than the bulk Ge-Ge bond length.[9]

In this letter, we report on EXAFS experiments of implanted Ga in Ge to investigate the lattice location of the Ga atoms and the local environment around the impurity. These experiments are corroborated with density functional theory (DFT) calculations and 4-point-probe (4PP) sheet resistance measurements to determine the electrically active Ga fraction.

^{69}Ga has been implanted in a 1.8 μm nominally undoped (100)-Ge layer, grown on a Si substrate by chemical vapor deposition. Implantations were performed at 250 °C to avoid amorphization, as confirmed by ion channeling experiments (not shown). An inclination angle of 10° with respect to the sample surface was used to minimize channeling during implantation. Three different energies (2.6 MeV, 1.5 MeV, and 825 keV) and relative fluences of 54%, 27%, and 19% were used to create a homogeneous Ga distribution over a depth of 0.2–1.5 μm. Five different total fluences were implanted, from 2.9×10^{14} to 2.9×10^{16} atoms/cm^2, corresponding to Ga concentrations of 2.2×10^{18}/cm^3 (0.005 at. %), 6.6×10^{18}/cm^3 (0.015 at. %), 2.2×10^{19}/cm^3 (0.05 at. %), 6.6×10^{19}/cm^3 (0.15 at. %), and 2.2×10^{20}/cm^3 (0.5 at. %).

To study such low concentration samples with fluorescence EXAFS, further processing was required to achieve an optimum signal-to-noise ratio. We performed a *lift-off* procedure to separate the Ga-implanted Ge layer from the Si substrate. After mechanical grinding of the Si substrate to 30 μm, the sample was placed in a KOH-solution for 48 h,

a)Electronic mail: stefandecoster@hotmail.com.

which selectively etched the Si substrate without affecting the Ge layer. The lift-off layers were then mounted on adhesive Kapton, and several such films were stacked together to increase the total number of absorbers and hence the fluorescence signal. Moreover, elastic scattering and diffraction from the substrate layer were eliminated by the lift-off procedure. More information on the lift-off protocols for a thin film of Ge and other semiconductor materials is presented in Ref. 10.

Fluorescence EXAFS experiments were performed at the x-ray absorption spectroscopy beamline at the Australian Synchrotron, measuring at the Ga K-edge (10367 eV) with the samples maintained at 18 K. A 100-element solid state Ge detector, positioned at 90° with respect to the incoming x-ray beam, was used in combination with a Zn filter between the sample and the detector to reduce the elastic scattering incident on the detector. Background subtraction, data processing, and fitting were performed with the ATHENA and ARTEMIS programs within the IFEFFIT 1.2.11 c package.[11,12] Data were recorded up to a photoelectron wavenumber k of 14 Å^{-1} (where the Ge K-edge appears) while the Fourier transform (FT) of the normalized EXAFS oscillations was performed over a k-range of $2.2 - 11 \text{ Å}^{-1}$, using a Hanning window with a width of 0.5 Å^{-1}.[13,22,23]

The k^2-weighted EXAFS as a function of photoelectron momentum and the magnitude of the FT of the isolated fine structure as a function of non-phase corrected radial distance is shown in Figs. 1(a) and 1(b), respectively, for the five different Ga concentrations. The data have been offset vertically for clarity. Clearly, the Ga impurities are embedded in a highly ordered matrix. To fit the data, a backward FT was performed for a non-phase corrected radial distance range of 1.60–4.65 Å, using a Hanning window with a width of 0.3 Å,
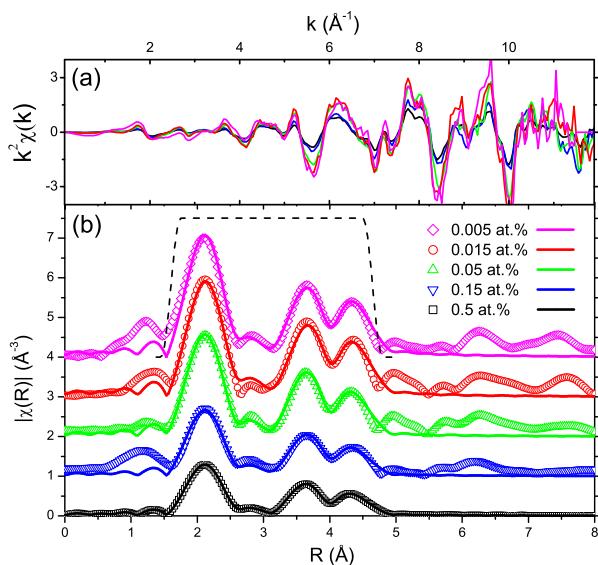
as shown by the dashed line in Fig. 1. *Ab initio* calculations (feff8[14]) were used to determine the backscattering amplitude and phase shifts of the single and multiple scattering (MS) paths, for a Ga absorber on a substitutional site in a Ge matrix, as shown in Table I. The single scattering (SS) path lengths were taken as independent variables, and to reduce the number of fit variables, we calculated the MS path lengths from the SS path lengths using trigonometry and the first order approximation that the first and second nearest neighbor displacements are only radial. Three different Debye-Waller factors (DWFs) σ^2 were used for the SS paths, and the DWFs for the MS paths were approximated from these values.[15,24] An SO_2-value of 1.1 was extracted from a multiple fit of the three lowest Ga concentrations with the coordination numbers set to the values in Table I, and kept constant for the remainder of the fitting process. The energy threshold E_0 was a fit variable to accommodate the anticipated change in Fermi energy as a function of Ga concentration.

For Ga concentrations ≤ 0.05 at.%, a good fit is obtained by assuming all Ga impurities are substitutional in the Ge matrix. The fits are represented by the solid lines in Fig. 1(b), the fitting parameters are tabulated in Table II, and the NN distances and DWFs as a function of Ga concentration are shown in Figs. 2 and 3, respectively. The fitted DWFs of roughly 0.003 Å^2 are slightly larger than typical values for a bulk undoped Ge crystal (0.002 Å^2), consistent with a doped lattice. The small R-factors for these three fits indicate the high quality of the fit and support the model of perfectly substitutional Ga atoms in Ge. From 4PP measurements, we have extracted the electrically active Ga fraction, assuming a homogeneously implanted layer of 1.5 μm and a concentration-dependent mobility in Ga-doped Ge to account for ionized impurity scattering.[16] Although the EXAFS experiments indicate the majority of Ga atoms occupies a substitutional site, we measured an active fraction of roughly 50% for Ga concentrations up to 0.05 at. %, consistent with the presence of compensating defects, as expected without post-implantation thermal annealing.

At higher Ga concentrations (0.15 at. % and 0.5 at. %), a reduction in amplitude of the FT of the oscillations is observed (Fig. 1(b)). When fitting these data with the same model (all Ga atoms are substitutional), the fit quality

FIG. 1. Spectra of (a) k^2-weighted EXAFS as a function of photoelectron momentum and (b) the magnitude of the Fourier transform (open symbols) as a function of non-phase corrected radial distance for Ga atoms in a bulk Ge matrix for different Ga concentrations. The solid lines represent the best fit to the experimental data, assuming that all Ga atoms are on substitutional Ge sites for the three lowest Ga concentrations, and allowing a non-substitutional fraction for the two highest concentrations. The dashed line represents the Hanning window from 1.60 to 4.65 Å with a width of 0.3 Å used for the backward FT in the fitting procedure. The data have been offset vertically for clarity.

TABLE I. Single and multiple scattering paths used in the fitting model for substitutional Ga in Ge, including the degeneracy (N), the amplitude (amp), the radial displacement (Δr), and the EXAFS Debye-Waller factor (σ^2) for each path; the absorbing Ga atom and the first, second, and third nearest neighbor Ge atoms are labeled as [+], Ge_1, Ge_2, and Ge_3, respectively.

Nr	Path	N	Amp	Path length (Å)	σ^2
1	$[+] \, Ge_1 \, [+]$	4	100.0	$2.449 + \Delta r_1$	σ_1^2
2	$[+] \, Ge_2 \, [+]$	12	94.0	$3.999 + \Delta r_2$	σ_2^2
3	$[+] \, Ge_1 \, Ge_1 \, [+]$	12	6.9	$4.448 + 1.87 \Delta r_1$	$2\sigma_1^2$
4	$[+] \, Ge_2 \, Ge_1 \, [+]$	24	31.0	$4.448 + 0.33 \Delta r_1$ $+ 0.91 \Delta r_2$	σ_2^2
5	$[+] \, Ge_3 \, [+]$	12	61.0	$4.689 + \Delta r_3$	σ_3^2
6	$[+] \, Ge_1 \, [+] \, Ge_1 \, [+]$	4	4.6	$4.898 + 2\Delta r_1$	$4\sigma_1^2$
7	$[+] \, Ge_1 \, Ge_2 \, Ge_1 \, [+]$	12	4.3	$4.898 + 0.67\Delta r_1$ $+ 0.82\Delta r_2$	$\sigma_1^2 + \sigma_2^2$

TABLE II. Fitting parameters for the different Ga concentrations [Ga], assuming substitutional Ga in Ge: first, second, and third nearest neighbor distances r_1, r_2, and r_3; EXAFS Debye-Waller factors σ_1^2, σ_2^2, and σ_3^2 for the single scattering paths; the R-factor, representing the quality of the fit; best fit E_0-values and the fraction of substitutional Ga atoms f_S.

[Ga] (at. %)	r_1 (Å)	r_2 (Å)	r_3 (Å)	σ_1^2 (Å^2)	σ_2^2 (Å^2)	σ_3^2 (Å^2)	R-factor	E_0 (eV)	f_S (%)
0.005	2.418 ± 10	4.002 ± 17	4.678 ± 22	0.0030 ± 7	0.0049 ± 13	0.0048 ± 19	0.013	7.7 ± 2.0	100
0.015	2.429 ± 6	4.008 ± 9	4.690 ± 12	0.0033 ± 4	0.0046 ± 16	0.0050 ± 9	0.019	8.1 ± 1.1	100
0.05	2.421 ± 5	3.996 ± 7	4.673 ± 10	0.0044 ± 3	0.0055 ± 5	0.0068 ± 9	0.007	7.7 ± 0.8	100
0.15	2.424 ± 6	4.004 ± 9	4.688 ± 13	0.0036 ± 9	0.0046 ± 5	0.0062 ± 15	0.019	7.5 ± 1.1	58.8
	2.429 ± 9[a]	4.006 ± 14[a]	4.677 ± 20[a]	0.0075 ± 7[a]	0.0082 ± 11[a]	0.0098 ± 20[a]	0.054[a]	7.6 ± 1.3[a]	100[a]
0.5	2.427 ± 3	3.997 ± 5	4.674 ± 7	0.0041 ± 5	0.0054 ± 5	0.0065 ± 8	0.010	6.7 ± 0.8	48.7
	2.436 ± 11[a]	4.001 ± 17[a]	4.680 ± 24[a]	0.0097 ± 10[a]	0.0101 ± 14[a]	0.0118 ± 25[a]	0.080[a]	7.0 ± 0.6[a]	100[a]

[a]These fitting parameters have been obtained, fixing the substitutional Ga fraction during the fit to 100%.

decreases and significantly increased DWFs are required to account for the amplitude reduction, apparent in Fig. 3. These results indicate that a fraction of Ga atoms is in a defective environment. To estimate the substitutional fraction, we have fitted the data with two components: one representing substitutional Ga atoms, the other representing Ga atoms in various defective environments such that the contribution of this fraction to the isolated EXAFS amplitude is negligible (as could result from a large variation in NN distances and, as a consequence, high DWF). For this model, we multiplied the coordination number of all paths with the same variable f_S (substitutional fraction). A much improved fit was obtained, as is obvious from the significantly reduced R-factors in Table II, with substitutional fractions of 60% and 50% for Ga concentrations of 0.15 at. % and 0.5 at. %, respectively. This decrease in substitutional Ga fraction is consistent with a twofold decrease in the electrically active fraction inferred from 4PP measurements. The fitted NN distances and DWFs for this model are represented by filled symbols in Figs. 2 and 3, respectively, and are comparable to the fitted values for lower Ga concentrations, supporting the validity of this model. Other models including a Ga metal fraction or specific defect configurations (such as a

Ga-vacancy complex) were tested, but did not result in an improved fit.

For the Ga concentrations used in this study, the first, second, and third NN distances are not influenced by the Ga concentration (Fig. 2). When comparing to values measured for an unimplanted Ge layer on Si (dashed lines in Fig. 2), as obtained from high resolution x-ray diffraction measurements, we conclude that local strain around the implanted Ga impurities is limited to the first NN, inducing a relative lattice contraction of roughly 1%. The second and third nearest NN distances are, within experimental error, similar to the pristine Ge values. These results have been compared with density functional theory calculations,[17] using the APW + lo method,[18] as implemented in the WIEN2K code[19,20] and the Perdew-Burke-Ernzerhof functional.[21] Ga was positioned on a substitutional site in a $2 \times 2 \times 2$ super-cell, containing 64 atoms. These calculations showed that the first NN distance of a Ga atom in a Ge matrix is 1.25% smaller compared to bulk Ge, while the second and third NN distances are only 0.21% and 0.20% smaller, respectively, in agreement with our observations.

In conclusion, we have demonstrated that it is possible to perform accurate lattice location experiments in a very dilute system by means of EXAFS. At low Ga concentrations
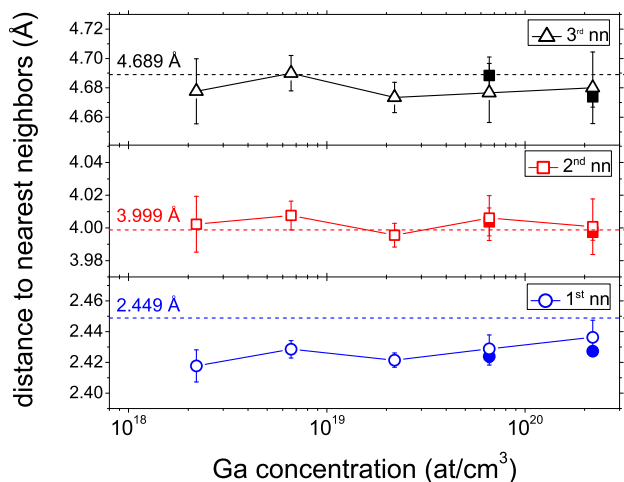

FIG. 2. The best fit distance to the first (circles), second (squares), and third (triangles up) nearest neighbors of substitutional Ga in Ge as a function of Ga concentrations. The dashed lines represent the NN distances in an unimplanted Ge layer on Si, as determined with high resolution x-ray diffraction measurements. The open symbols represent the fitting model with all Ga atoms on the substitutional site, the solid symbols represent the model with a variable fraction of substitutional Ga atoms.
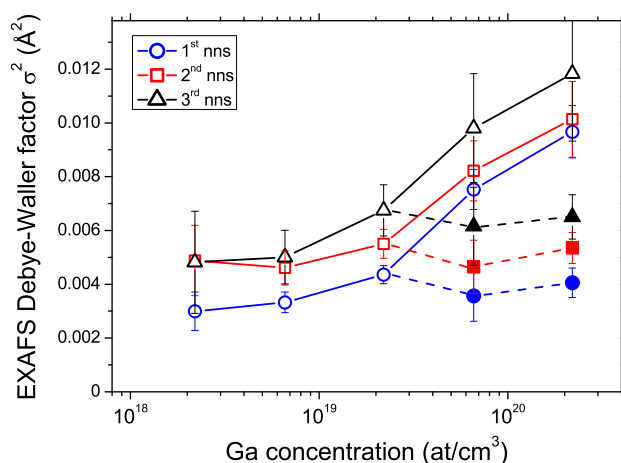

FIG. 3. The fitted EXAFS Debye-Waller factors for the first (circles), second (squares), and third (triangles) single scattering path of substitutional Ga absorbers in a Ge crystal matrix as a function of Ga concentration, assuming that all (open symbols) or only a fraction (solid symbols) of the Ga dopants are on substitutional sites.

(≤ 0.05 at.%), the majority of the Ga atoms are substitutional after ion implantation at elevated temperature ($250\,^\circ$C). Without post-implantation thermal annealing, we measured a sheet resistance consistent with an electrically active fraction of 50%, indicating the presence of compensating defects. At higher Ga concentrations (≥ 0.15 at.%), the fraction of Ga atoms on a substitutional site decreases to 50%–60%, with the remainder in defective environments. Finally, the introduction of Ga atoms in Ge results in a first nearest neighbor lattice contraction of 1% surrounding the impurity, while second or higher nearest neighbor distances are fully relaxed, in agreement with density functional calculations.

[1]E. Simoen and C. Claeys, *Germanium-Based Technologies: From Materials to Devices* (Elsevier, Amsterdam, 2007).

[2]G. Hellings, C. Wuendisch, G. Eneman, E. Simoen, T. Clarysse, M. Meuris, W. Vandervorst, M. Posselt, and K. De Meyer, Electrochem. Solid-State Lett. **12**, H417 (2009).

[3]V. Heera, A. Mücklich, M. Posselt, M. Voelskow, C. Wündisch, B. Schmidt, R. Skrotzki, K. H. Heinig, T. Herrmannsdörfer, and W. Skorupa, J. Appl. Phys. **107**, 053508 (2010).

[4]G. Impellizzeri, S. Mirabella, A. Irrera, M. G. Grimaldi, and E. Napolitani, J. Appl. Phys. **106**, 013518 (2009).

[5]N. Ioannou, D. Skarlatos, N. Z. Vouroutzis, S. N. Georga, C. A. Krontiras, and C. Tsamis, Electrochem. Solid-State Lett. **13**, H70 (2010).

[6]T. Herrmannsdörfer, V. Heera, O. Ignatchik, M. Uhlarz, A. Mücklich, M. Posselt, H. Reuther, B. Schmidt, K.-H. Heinig, W. Skorupa, M. Voelskow, C. Wündisch, R. Skrotzki, M. Helm, and J. Wosnitza, Phys. Rev. Lett. **102**, 217003 (2009).

[7]A. Mesli, L. Dobaczewski, K. Bonde Nielsen, V. Kolkovsky, M. Christian Petersen, and A. Nylandsted Larsen, Phys. Rev. B **78**, 165202 (2008).

[8]V. Kolkovsky, M. Christian Petersen, A. Mesli, J. Van Gheluwe, P. Clauws, and A. Nylandsted Larsen, Phys. Rev. B **78**, 233201 (2008).

[9]H. Höhler, N. Atodiresei, K. Schroeder, R. Zeller, and P. H. Dederichs, Phys. Rev. B **71**, 035212 (2005).

[10]S. Decoster, C. J. Glover, B. Johannessen, R. Giulian, D. J. Sprouster, P. Kluth, L. L. Araujo, Z. S. Hussain, C. Schnohr, H. Salama, K. Temst, A. Vantomme, and M. C. Ridgway, "Lift-off protocols for thin films for use in EXAFS experiments," J. Synchrotron Radiat. (to be published).

[11]M. Newville, J. Synchrotron Radiat. **8**, 322 (2001).

[12]B. Ravel and M. Newville, J. Synchrotron Radiat. **12**, 537 (2005).

[13]The limited k-range used for the FT is a consequence of the background subtraction which is impeded by the large concentration difference between the Ga impurities and the Ge matrix. Although resonant Raman scattering (RRS) is a low-probability event, it becomes significant when studying low concentrations of impurities (Ga) in a $Z + 1$ (Ge) matrix. The energy and intensity of the Ge RRS peak changes with incoming photon energy, and passes through the fixed energy window set on the Ga fluorescent x-rays, hence impeding an accurate background subtraction at high k, especially for the lowest Ga concentrations.

[14]A. L. Ankudinov, B. Ravel, J. J. Rehr, and S. D. Conradson, Phys. Rev. B **58**, 7565 (1998).

[15]To a first approximation, we assume that path 4 is a collinear MS path, as is path 6, which means that the DWFs can be calculated. Further approximations have been made for the triangular MS paths 3 and 7, assuming that the DWFs will be larger than the SS paths and smaller than the *ababa* MS paths.

[16]O. A. Golikova, B. Y. Moizhes, and L. S. Stil'bans, Sov. Phys. Solid State **3**, 2259 (1962).

[17]P. Hohenberg and W. Kohn, Phys. Rev. **136**, 864 (1964).

[18]E. Sjöstedt, L. Nordström, and D. J. Singh, Solid State Commun. **114**, 15 (2000).

[19]S. Cottenier, *Density functional theory and the family of (L) APW methods: a step-by-step introduction* (Instituut voor Kern-en Stralingsfysica, KU Leuven, Belgium, 2002), ISBN 90-807215-1-4, see http://www.wien2k.at/reg_user/textbooks.

[20]P. Blaha, K. Schwarz, G. Madsen, D. Kvasnicka, and J. Luitz, *User's guide, Wien2k 12.1* (Karlheinz Schwarz, Techn. Universität Wien, Austria, 1999), ISBN 3-9501031-1-2.

[21]J. P. Perdew, K. Burke, and M. Ernzerhof, Phys. Rev. Lett. **77**, 3865 (1996).

[22]H. J. Sánchez, M. C. Valentinuzzi, and C. Pérez, J. Phys. B **39**, 4317 (2006).

[23]S. Medling and F. Bridges, J. Synchrotron Radiat. **18**, 679 (2011).

[24]P. Shanthakumar, M. Balasubramanian, D. M. Pease, A. I. Frenkel, D. M. Potrepka, V. Kraizman, J. I. Budnick, and W. A. Hines, Phys. Rev. B **74**, 174103 (2006).